A Study on the Smearing and Slip Behaviour of Radial Cylindrical Roller Bearings

Dr. Bruno Johannes Scherb

INA WÄLZLAGER SCHAEFFLER oHG

Prof. Dr. Jürgen Zech

Georg-Simon-Ohm-Fachhochschule Nürnberg

Abstract

Knowledge of the features and qualities of a machine element are essential foundations for its successful operation. High grade materials, more accurate calculation methods and modern manufacturing processes lead to continuous design and performance improvements and hence increased power within minimised spatial requirements. INA cylindrical roller bearings, series SL 1923.., ZSL 1923.. and LSL 1923.. follow this trend and due to their high performance characteristics and low physical volume they have obtained a firm place as high performance machine elements.

Essential characteristics of radial cylindrical roller bearings are their behaviour regarding kinematics, noise, vibration, dynamic frictional torque, cage speed, speed of a rolling element, slip etc.

The paper gives details of the kinematic behaviour concerning the relationship between the roller set speed or the cage speed and the speed of a rolling element in connection with the occurrence of smearing.

This kind of damage occurs during the running in stage of a machine and is becoming very important because of the enormous costs which are caused by down time and lost production.

Keywords: cylindrical roller bearing, smearing, slip

ISSN 1616-0726 Sonderdruck Schriftenreihe der Georg-Simon-Ohm-Fachhochschule Nürnberg Nr. 5, Nürnberg 2001

0. SYMBOLS AND NOTATION

		UNITS
C	basic dynamic load rating	N
C_0	basic static load rating	N
d_R	roller diameter	mm
d_M	mean diameter	mm
F_r	radial load	N
F_a	axial load	N
J_R	rolling element mass moment of inertia	kg m^2
L	calculated bearing life time	h
L_{SL}	calculated bearing life time for SL bearing	h
M_A	driving torque of the test rig	Nm
M_R	frictional torque of the test bearing	Nm
M_{RA}	rolling element accelerating torque	Nm
N_{RB}	relative rolling element speed shortly before entering the load zone	–
N_{RE}	relative rolling element speed in the load zone	–
n_C	cage rotational speed	rpm, s^{-1}
n_G	limiting rotational speed of a bearing	rpm, s^{-1}
n_{IR}	inner ring rotational speed	rpm, s^{-1}
n_R	rolling element speed	rpm, s^{-1}
n_{RB}	rolling element speed shortly before entering the load zone	rpm, s^{-1}
n_{RE}	rolling element speed within the load zone	rpm, s^{-1}
n_{RS}	roller set speed	rpm, s^{-1}
P_{RA}	rolling element accelerating power	W
S_C	cage slip	%
S_{RB}	rolling element slip shortly before entering the load zone	%
S_{RE}	rolling element slip within the load zone	%
S_{RS}	roller set slip	%
t_{RA}	rolling element accelerating time	s
W_A	calculated local energy of acceleration friction energy	W

$_{work}$ working value
$_{kin}$ kinematic value
$_{meas}$ measured value

SL full complement radial cylindrical roller bearing
ZSL radial cylindrical roller bearing with plastic spacers
LSL radial cylindrical roller bearing with a brass disc cage
NJ radial cylindrical roller bearing with a brass window cage

1. INTRODUCTION

Modern radial cylindrical roller bearings, e.g. INA series SL 1923.., LSL 1923.. and ZSL 1923.. (figure 1) have an improved internal construction with a fundamentally higher load carrying capacity than conventional radial cylindrical roller bearings.

a) b) c)

Fig. 1: INA Cylindrical Roller Bearings series a) SL 1923, full complement radial cylindrical roller bearing
b) LSL 1923, radial cylindrical roller bearing with a brass disc cage
c) ZSL 1923, radial cylindrical roller bearing with plastic spacers

These extremely high load carrying capacities show themselves to be significant following consideration of the bearing working life [1].

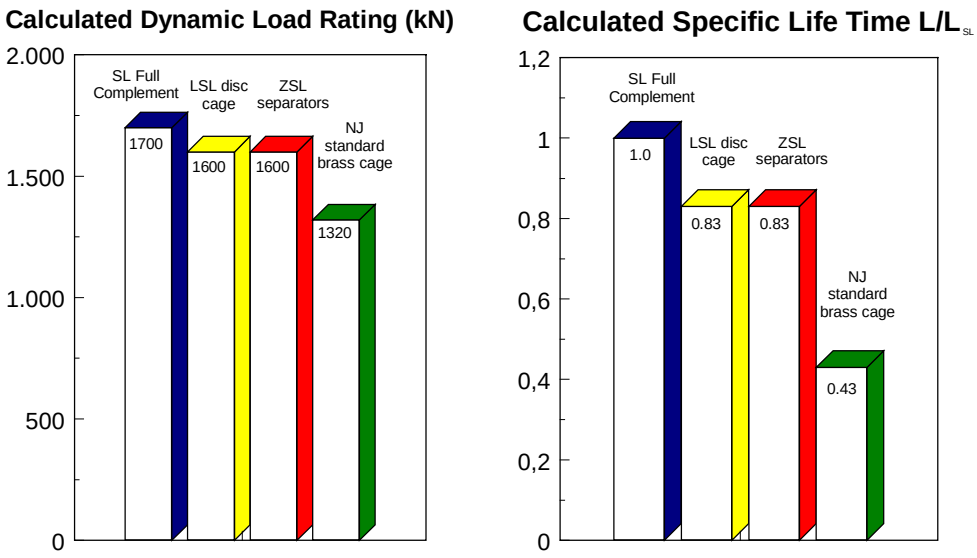

Fig. 2: Relative load carrying capacities and calculated respective lifetimes [10]

The calculation of the expected life of a roller bearing can lead to certain influential factors which go beyond the investigation into fatigue life. In such cases the occurrence of wear of the roller bearing as a function limiting characteristic becomes very important, thus types of wear which occur during the running in stage of a machine have been categorised as being especially critical.

One such fatigue failure type is well known as the concept of smearing and occurs predominantly under certain working conditions. This is especially true of cylindrical and spherical roller bearings with large dimensions where the sliding and slip conditions within the bearing lead to the occurrence of smearing.
Smearing is defined as the change of the surface area of a metallic roller sliding contact under relative motion due to the beginning of adhesive wear. Previous investigations on the topic smearing have been published by [2],[3], [4], [5], [6] and [7]. The reports [5], [6] and [7] investigated the single rolling element / bearing raceway contacts by running tests in an element test rig. As a result of these publications it was found that the smearing occurrence is related to certain conditions and connections within a bearing which are:

- fast deceleration and acceleration
- non stationary slip which means fluctuations in slip occurrence
- sliding under simultaneous Hertzian pressure
- breakdown of the carrying lubricant film with metal to metal contact between the rolling elements and the bearing ring raceways
- momentary bonding and welding with material transfer (adhesion wear)
  high mass moment of inertia of the rolling elements
- low loading

It was established that during rotation the rolling element ascribes at the entrance into the load zone a sliding motion by simultaneous occurrence of Hertzian pressure. At this point the carrying lubricant film breakdown and metal to metal contact occur which results in momentary bonding and welding with material transfer. Figure 3 illustrates the different speed zones within a radial bearing and the speed characteristic of a single rolling element during rotation.

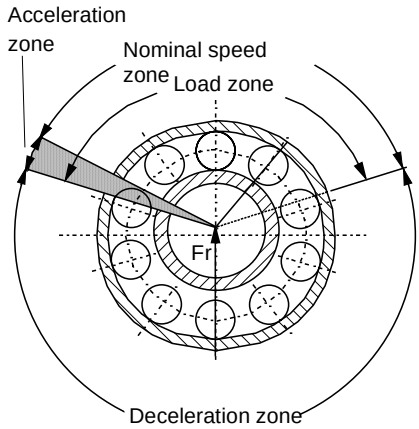

Fig. 3a: Speed zones in a radial bearing

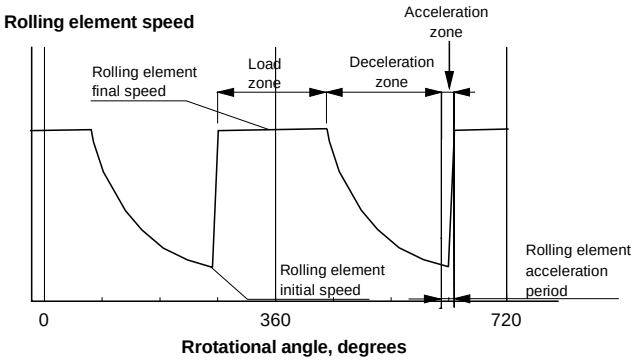

Fig. 3 b: Rotational speed charasteristic of a single rolling element

The rolling elements move through three different speed zones, which are the nominal speed zone located in the load zone of the bearing, the deceleration zone and the acceleration zone located at the beginning of the load zone (figure 3a). A typical rotational speed characteristic of a single rolling element is illustrated in figure 3b, where the different rotational speeds of a rolling element are shown.

The photographs of damage range from the smallest, where the material transfer is barely visible, to the large areas of scuff damage detected by macroscopic areas of removed material. These may lead to a bearing failure.
Figure 4 shows large surface smearing on the bearing raceways which are a) the outer ring raceway, b) the inner ring raceway and c) and d) the rolling element raceway of a cylindrical roller bearing, whereby d) show the smearing in detail from c).

a) outer ring raceway

b) inner ring raceway

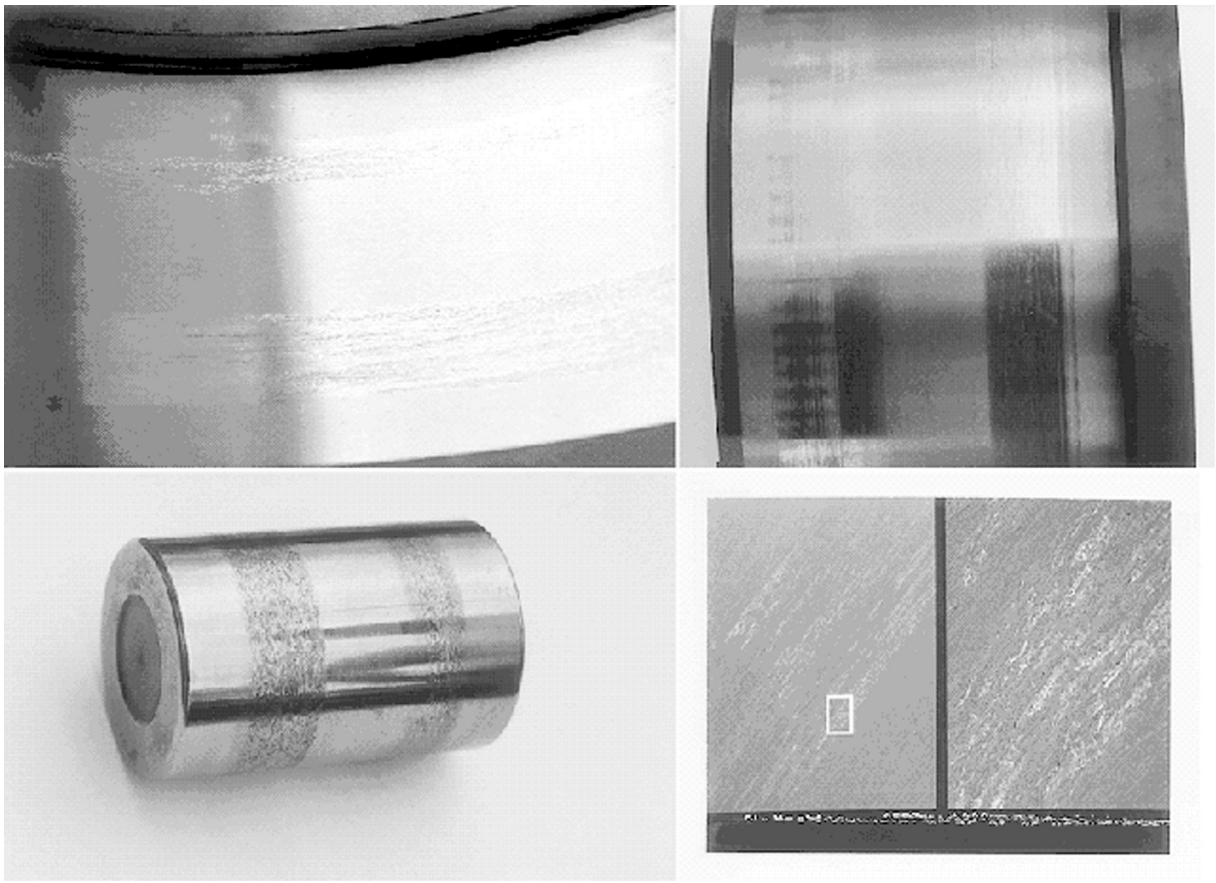

c) rolling element raceway

d) rolling element raceway in detail
the right photo show enlarged the section of the frame (left photo)

Fig. 4: Smearing of a cylindrical roller bearing

The damage type smearing has a number of economic consequences. This type of damage usually appears on new bearings after only a short running time. The early replacement, especially of large roller bearings, leads to considerable costs which are then compounded with down time and lost production costs.

2. TEST OBJECTIVES

In many applications roller bearings often experience very large fluctuations in their working conditions. The fluctuations are due to the operating time, speed, and the power flow through the machine, hence the frictional torque and kinematic behaviour of the bearing will also fluctuate.
Transient slip conditions have been associated with smearing through testing and applications, especially cylindrical roller bearings with rolling elements having a high moment of inertia. An understanding of the conditions in which in cylindrical roller bearings roller set or cage slip and slip of a rolling element occurs is important. This information gives the user the security that the running conditions of a cylindrical roller bearing under the given working conditions have been correctly assessed. Thus it is not certain that a cylindrical roller bearing running with slip will fail.

Surveys of cylindrical roller bearing applications showed that the smearing occurred on all large roller bearings. From the application failures it was possible to identify that the following influences lead to smearing:

- Fast acceleration and deceleration within the roller bearing
- Unsteady roller element slip
- High mass moment of inertia of the rolling elements
- Low loads
- Collapse of the load carrying lubricant film
- Sticking and welding due to material transfer

Tests were performed on radial cylindrical roller bearings SL 192332, ZSL 192332, LSL 192332 and NJ 2332 with a shaft diameter of 160 mm. The objectives were to examine the application limitations of these bearing types in respect of material transfer and to obtain possible influences of the running conditions of bearings exhibiting this type of damage.

Further objectives were to produce measurement data in order to verify a method for predicting the conditions for smearing and to test raceway coatings as a possible prevention of the occurrence of smearing.

3. THEORETICAL CONSIDERATIONS

3.1 Rolling Element Speed, Roller Set and Cage Speed

The kinematic rotational speed of a rolling element of a cylindrical roller bearing [9] have been calculated using equation (1).

$$n_R = -\frac{n_{IR}}{2} \cdot \left(\frac{d_M}{d_R} - \frac{d_R}{d_M} \right) \tag{1}$$

And for the roller set or cage rotational speed n_{RS} or n_C:

$$n_{RS} = n_C = \frac{n_{IR}}{2} \cdot \left(1 - \frac{d_R}{d_M} \right) \tag{2}$$

Hence the difference in the kinematic rotational speed gives the slip value of the rolling elements and roller set or cage according to the following equations:

$$S_C = \left(1 - \frac{n_{C,meas}\cdot}{n_{C,kin.}} \right) \cdot 100\% \tag{3}$$

$$S_{RE} = \left(1 - \frac{n_{RE,meas.}}{n_{Rkin.}} \right) \cdot 100\% \tag{4}$$

$$S_{RB} = \left(1 - \frac{n_{RBmeas.}}{n_{Rkin.}} \right) \cdot 100\% \tag{5}$$

Since the rolling elements, as a result of accelerations and decelerations, are subjected to rotational speed changes, a rolling element initial rotational speed n_{RB}, and a rolling element final rotational speed n_{RE}, are introduced by the authors. Thus the initial rotational speed of the rolling elements is the rotational speed immediately before entry to the load zone , and the end rotational speed is the speed of the rolling element in the load zone.
Following comparisons from further tests with other bearing types and sizes, the rolling element initial and final rotational speeds has been referred to the respective kinematic speed.

The following dimensionless equations are introduced by the authors:

$$N_{RE} = \frac{n_{RE}}{n_{R,kin.}} \quad \text{and} \tag{6}$$

$$N_{RB} = \frac{n_{RB}}{n_{R,kin.}} \tag{7}$$

3.2 Rolling Element Acceleration Torque and Acceleration Power

Using the difference in the rolling element initial and final rotational speeds, the rolling element accelerating time and the mass moment of inertia of the rolling elements, the equation for the rolling elements accelerating torque approximates to:

$$M_{RA} \approx J_R \cdot \dot{\omega} = J_R \cdot \left(\frac{n_{RE} - n_{RB}}{t_{RA}} \right) \tag{8}$$

And the rolling element accelerating power approximates to:

$$P_{RA} = -M_{RA} \cdot \left(n_{RE} - n_{RB} \right) = J_R \cdot \left(n_{RE} - n_{RB} \right)^2 \cdot \frac{1}{t_{RA}} \tag{9}$$

3.3 Correlation between roller set or cage and rolling element speed

Kinematic running of a cylindrical roller bearing means there is one well known relationship between the inner ring, roller set or cage and the rolling element speed. This relationship has been derived from the rolling relationship at the contact points of the rolling element with the inner ring and the rolling elements with the outer ring [9].
Running the roller bearing with either a cage or a roller set slip means that the rolling elements can no longer correctly roll kinematically on either the inner or the outer ring. Thus there exists, at least at one of these contacts, slip which means a speed difference between the contacts occurs.
Therefore it follows that the kinematic rolling element speed n_{Rkin} and the kinematic roller set speed n_{RS} or cage speed n_C can be calculated using the measured inner ring speed $n_{IR,meas}$ and the geometry of the test bearing.

Using the equations from [9] the following relationships have been derived by the authors:

$$n_{Rkin} = \frac{n_{IR,meas.}}{2} \left(\frac{d_M}{d_R} - \frac{d_R}{d_M} \right) \tag{10}$$

$$n_{c,kin.} = \frac{n_{IR,meas.}}{2}\left(1-\frac{d_R}{d_M}\right) \tag{11}$$

Since the running of the rolling elements in the load zone depends on the outer load it is possible to establish a calculated inner ring working speed using the measured rolling element final speed in the load zone. This is calculated as follows:

$$n_{RE,meas.} = -\frac{n_{IR,work}}{2}\left(\frac{d_M}{d_R}-\frac{d_R}{d_M}\right) \tag{12}$$

Using equation (6) for the relative rolling element final speed which is introduced by the authors and follow a simple rearrangement and substitution of equation (12), the calculated inner ring working speed becomes:

$$n_{IR,work} = n_{IR,meas.} \cdot N_{RE} \tag{13}$$

The roller set or cage speed now follows:

$$n_{RS,work} = n_{C,work} = \frac{n_{IR,work}}{2}\left(1-\frac{1}{d_M / d_R}\right) \tag{14}$$

Likewise, using equation 3, the inner ring working rotational speed can be used as a base to calculate the roller set or cage slip. Both of these can be compared to the measured slip value.

$$S_{C,work} = \left(1-\frac{n_{C,work}}{n_{C,kin}}\right)\cdot 100\% \tag{15}$$

4. EXPERIMENTAL WORK

4.1 The Test Rig

A large bearing test rig has been used to conduct these tests. The fundamental reasons for designing and building this test rig were to enable easy access to the test bearings to allow optimum sensor application and increased observations through the use of stroboscopes with video recording or high speed camera facilities. Furthermore a definite measurement of the test bearing frictional torque, without external influences, was necessary. The influence of the load direction, in the line of gravity, against gravity or any intermediate position, along with the superposition of an axial force was also required. All these requirements lead to the test rig shown in figure 5.

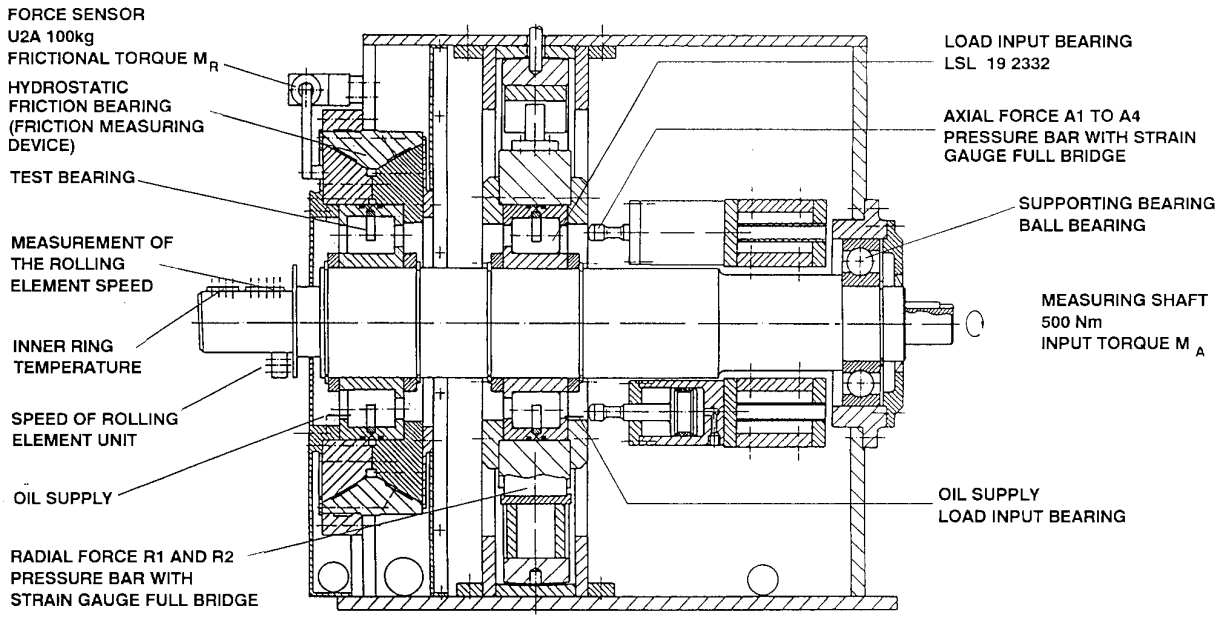

Fig. 5: Large Bearing Test Rig

The test bearing is housed on a floating support. Values for the rotational speed of the rolling element set or cage speed and the single rolling elements are obtained via a slip ring sensor mounted on the shaft sending a signal to the amplifier.
The test bearing is mounted on a hydrostatic support where the radial and axial forces are applied and the frictional torque is measured. It is due to the hydrostatic support that the exclusive measurement of the frictional torque is possible. The test bearing is loaded via the central bearing unit which in turn is loaded by means of a servo -hydraulically controlled pressure cylinder.
This allows a controlled test bearing load to be applied which can be maintained even through extreme temperature differences. The central bearing unit with the load cylinders may be rotated through 360 ° allowing the load zone to be varied accordingly. The axial load is applied to the test bearing via four servo - hydraulically controlled pistons acting on the stationary outer ring of the load input bearing located in the middle part, thus setting up an axial force in the shaft, and hence loading the test bearing. Another application of the pressure cylinders allows the simulation of an uneven axial load distribution within the test bearing. Constant lubricant viscosities across broad temperature ranges are guaranteed due to the use of powerful oil coolers and heaters. The speed regulated DC - motor allows measurements to be taken up to 4000 rpm.

4.2 Test Procedure

Extensive testing of kinematics and friction torque behaviour of full complement and cage guided bearings have been carried out. In order to investigate the effects of smearing and to derive a correlation to slip characteristics the sensor layout shown in figure 6 was developed by the authors.

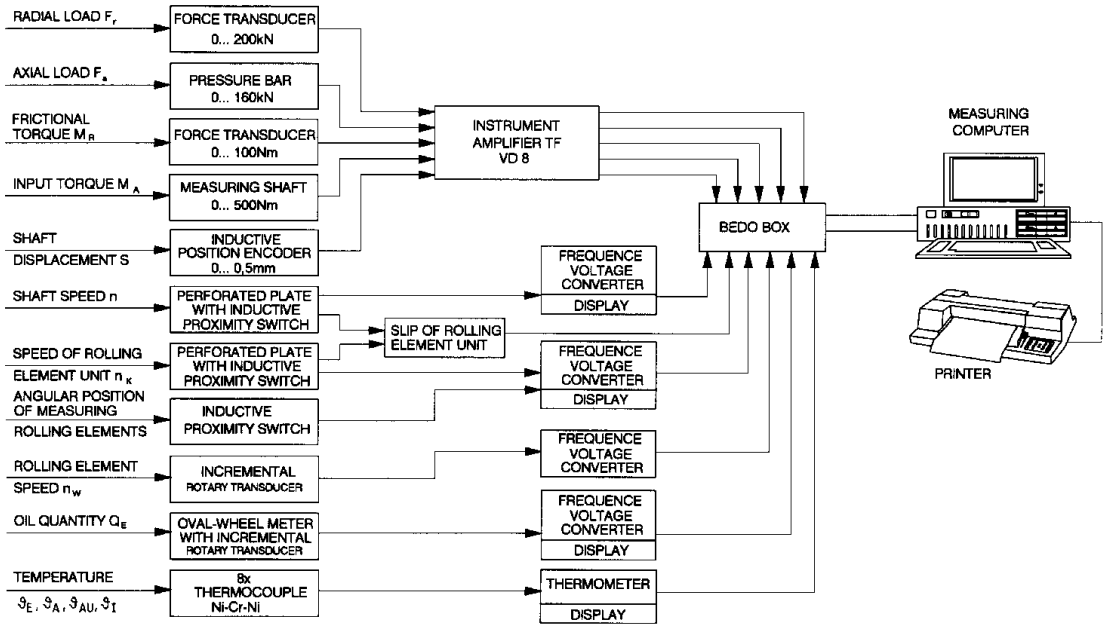

Fig. 6: Measuring chain with sensory analysis and monitoring equipment

The most important parameters which are to be considered for the evaluation of the characteristics and the early recognition of smearing are:

- the friction torque and its dynamic behaviour
- the kinematic behaviour with slip and speed characteristics
- the shaft displacement behaviour
- the vibrational behaviour
- the running noise behaviour

The measuring techniques developed for these tests, along with the transducers and signal layout, are shown in figure 7.

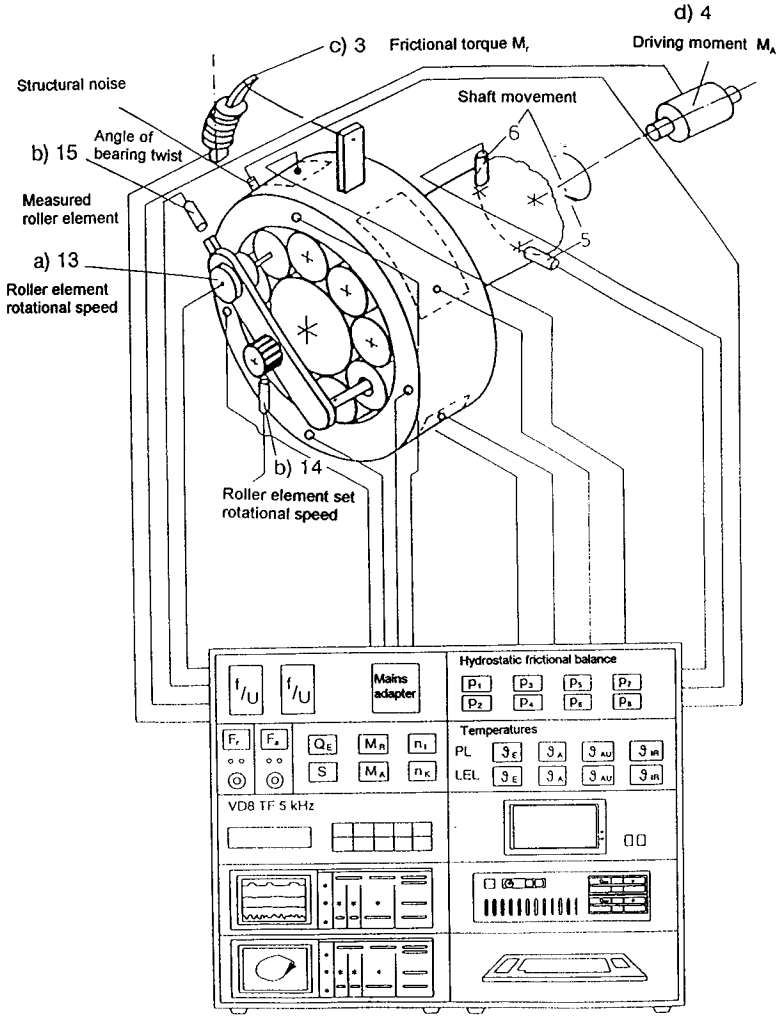

Fig. 7: Sensor layout for measuring bearing kinematics

During the tests it was possible to measure the frictional torque, the shaft displacement behaviour and the vibrational and running noise behaviour, although it was not possible to draw any conclusions as to the early recognition of material transfer. Thus the kinematic behaviour of the bearings is the only characteristic left requiring further examination. This refers to:

the rolling element set or cage rotational speed and associated slip
the rolling element rotational speed and associated slip
the rolling element acceleration moment
the rolling element acceleration power
the correlation between set, cage and rolling element rotational speed and associated slip

For the recording of the rotation of an individual rolling element, an incremental shaft encoder with a low mass moment of inertia and very low internal friction was used, and was coaxially connected to the rolling element with an universal joint. The incremental shaft encoder was thus connected to a disc rotating about the main shaft, which in turn is driven by one of the rolling elements remote from the other rolling elements. The disc, which gives the rotational speed of the rolling set or cage, has holes which, with the aid of an inductive proximity switch, give a measure of the rotational speed of the rolling element set or the cage. This signal from the incremental shaft encoder leads directly to a signal converter where the altered voltage signal is an instantaneous measure of the rotational speed of the individual rolling element. Through a further hole in the disc, which rotates with the rotational speed of the rolling element set or the cage speed, the angular position of the meas-

ured rolling elements is obtained, and with the aid of a stationary inductive proximity switch the angle of the measured rolling element is localised.

5. RESULTS AND DISCUSSION

5.1 Kinematics of a Cylindrical Roller Bearing

5.1.1 Influence of Bearing Design and Load Direction

It was established using the test facilities at INA that rolling elements within roller bearings do not always rotate with their nominal kinematic rotational speed but are subjected to alternating accelerations and decelerations. The various load zones within a roller bearing are shown in figure 3a.

The rolling elements only experience enough load in the load zone to assume a their kinematic rotation around their reference axis. In the decelerating zone the rolling elements slow down due to inertial friction until they enter the accelerating zone where they are accelerated to their nominal kinematic rotational speed due to the occurrence of a frictional force at the outer and inner ring contacts. The pattern of the accelerating and decelerating zones repeats itself periodically [10]. However with a low outer ring load the rolling elements in the load zone start to slip, i.e. they do not reach their nominal kinematic rotational speed. The result of this is rolling element set or cage slip.
The rolling elements are accelerated to their kinematic rotational speed from their starting speed within milliseconds of entering the load zone.

Figure 8 shows the rotational speed of a rolling element in relation to its relative position in a cylindrical roller bearing for different bearing designs. One further, not insignificant, influence on the rolling element speed is the load direction which is clearly visible in figure 9.

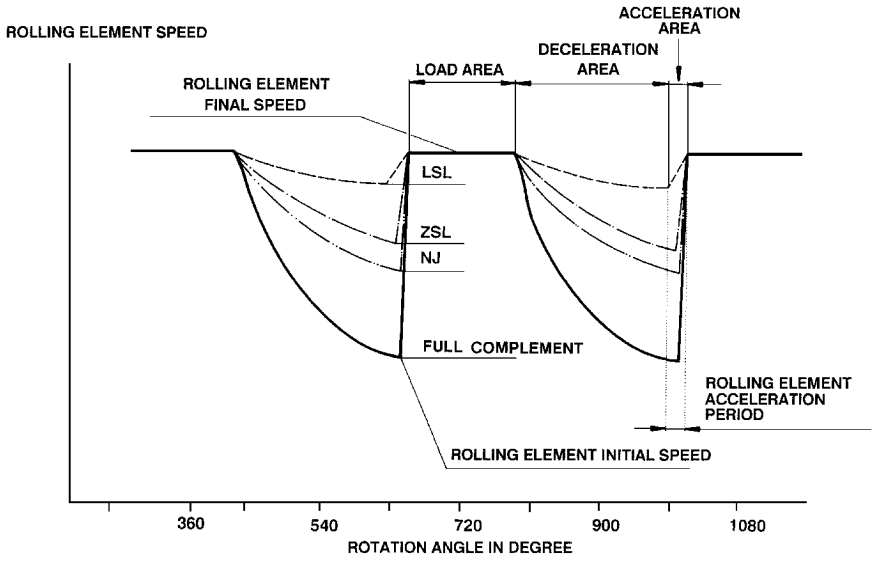

Fig. 8: Speed characteristics of the rolling elements for different bearing designs – load applied vertically (load zone above)

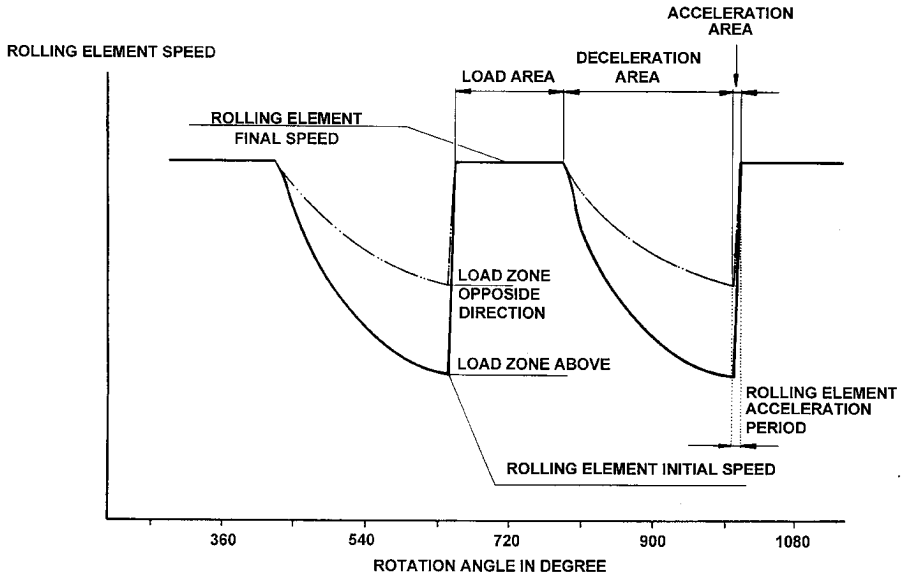

Fig. 9: Speed characteristics of the rolling elements for different load directions for bearing type SL 192332

The slip that the rolling elements experience can be up to 100% in extreme circumstances, this means that the rolling elements in the unloaded zone may decelerate until they reach the stationary point without any rotation of the rolling element. At the same time the maximum rolling element slip is influenced by the internal friction of the bearing at the contact points, i.e. roller - rib, roller - roller, roller - cage, and by the lubricant friction properties.

5.1.2 Rolling Element, Cage and Roller Set Speed

The evaluation of the measured diagrams (see figure 8) lead to the diagrams shown in figures 10 and 11. These figures show the results of the measured rolling element kinematics (see figure 9) dependent on the applied radial load for two bearing designs, e.g. full complement bearings (series SL) and brass disc cage bearings (series LSL).
These figures are achieved for each rotational speed and radial load by taking the initial speed of the rolling element n_{RB} and the rolling element speed within the load zone n_{RE} in relation to the calculated kinematic speed of the rolling element n_{Rkin}. The dotted lines show the relative rolling element speeds N_{RE} within the load zone, the straight lines show the relative rolling element speeds N_{RB} at the beginning of the acceleration zone.
It was found that the initial rotational speed is higher for cage guided bearings. Furthermore it was found that the brass disc cage bearings series LSL show the best results.
Figure 12 illustrates the roller set or cage slip for different bearing designs, exemplarily for an applied radial load of 5kN. As it can be seen the lowest slip values were achieved for the LSL bearing.

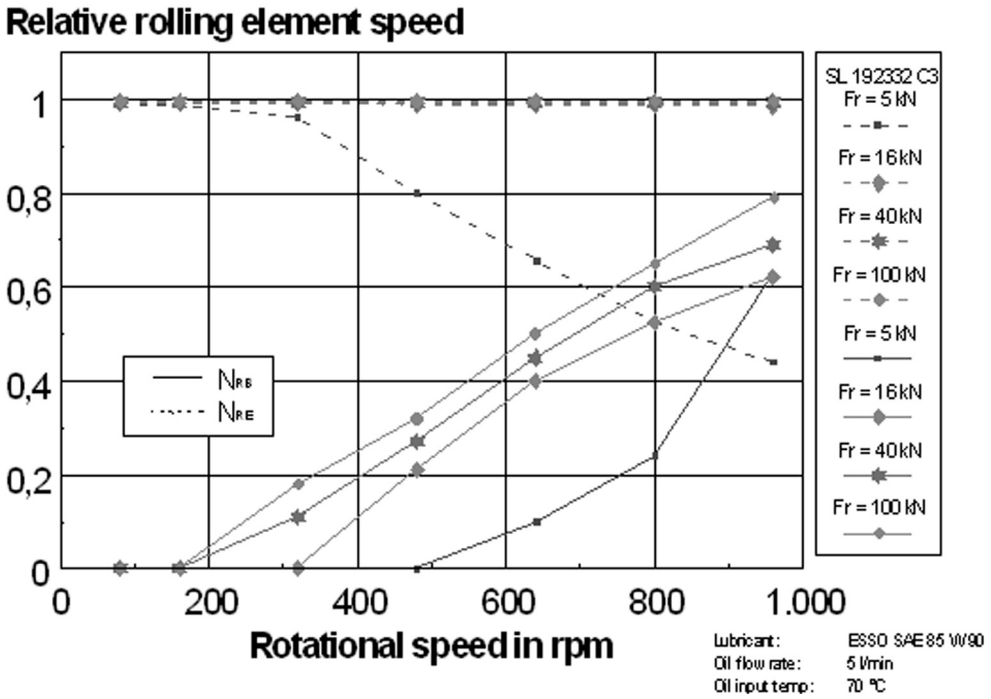

Fig.10: Relative rolling element rotational speed - SL 192332

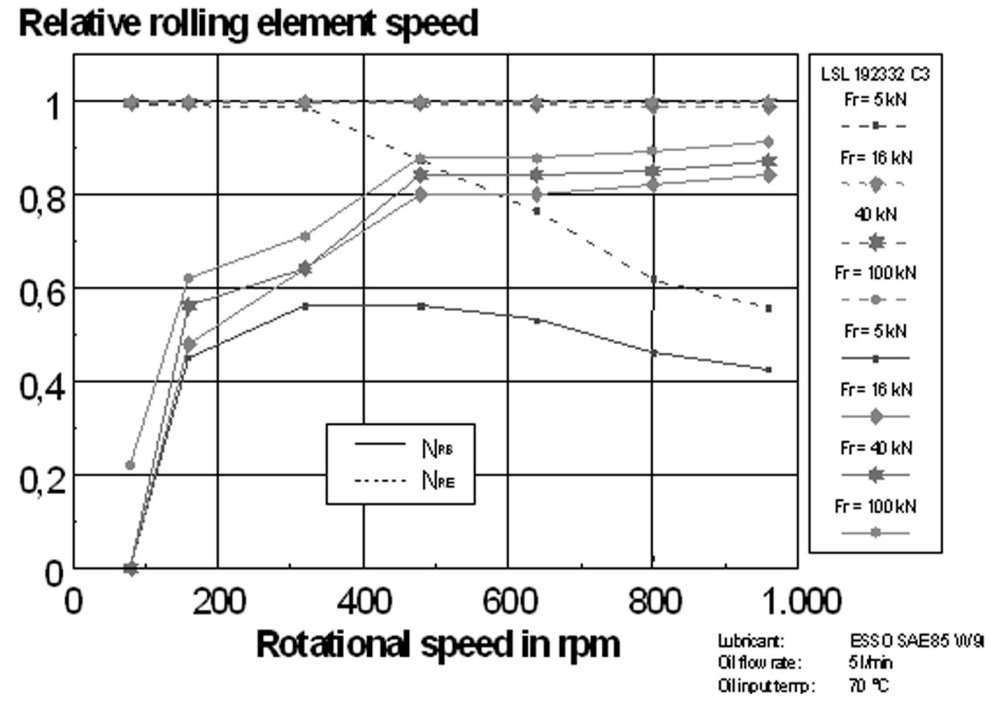

Fig. 11: Relative rolling element rotational speed - LSL 192332

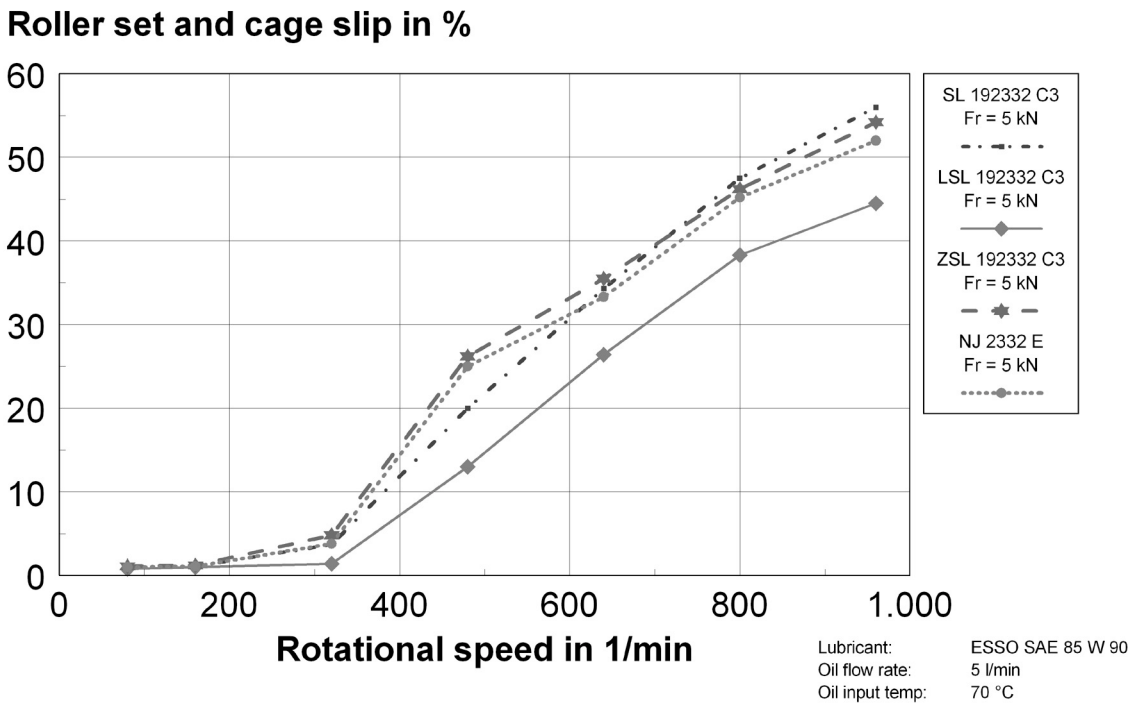

Fig.12: Rolling element set and cage slip

5.1.3 Rolling Element Acceleration Torque and Acceleration Power

For a certain load ratio ($C_0/F_r \leq 100$) the rolling elements experience enough force to almost achieve their kinematic rotational speed in the load zone. Reducing the outer load to $C_0/F_r > 100$ results in the rolling elements no longer achieving their kinematic rotational speed target and is accompanied by rolling element slip at the outer ring.
The tested cylindrical roller bearings show significantly variable rolling element rotational speed characteristics because of the different internal construction of the test bearings. These significant differences have also been measured for the slip values of the roller element sets or the cages (figure 12).
Using the rolling element acceleration time evaluated from the rotational speed gradient (figure 8) and the rolling element speed difference between the speed in the load zone and the speed entering the load zone (figure 10 and 11) the rolling element accelerating torque and power is calculated using equations 8 and 9. These results can be seen in figures 13 and 14 to be dependent upon the radial load and rotational speed.

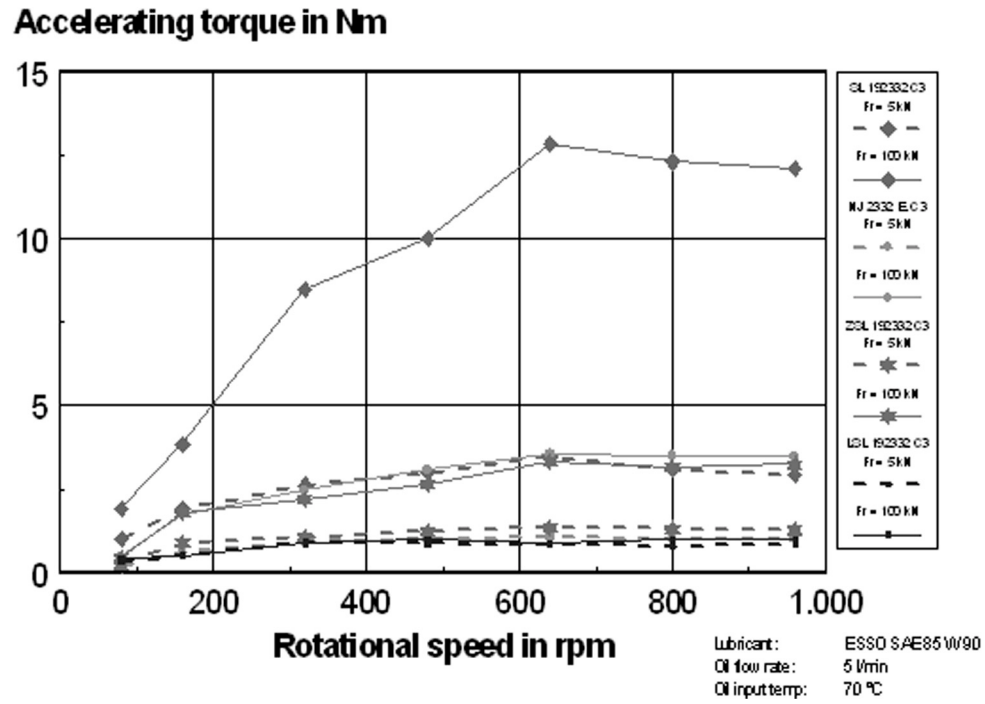

Fig. 13: Acceleration torque of a rolling element (equation 8)

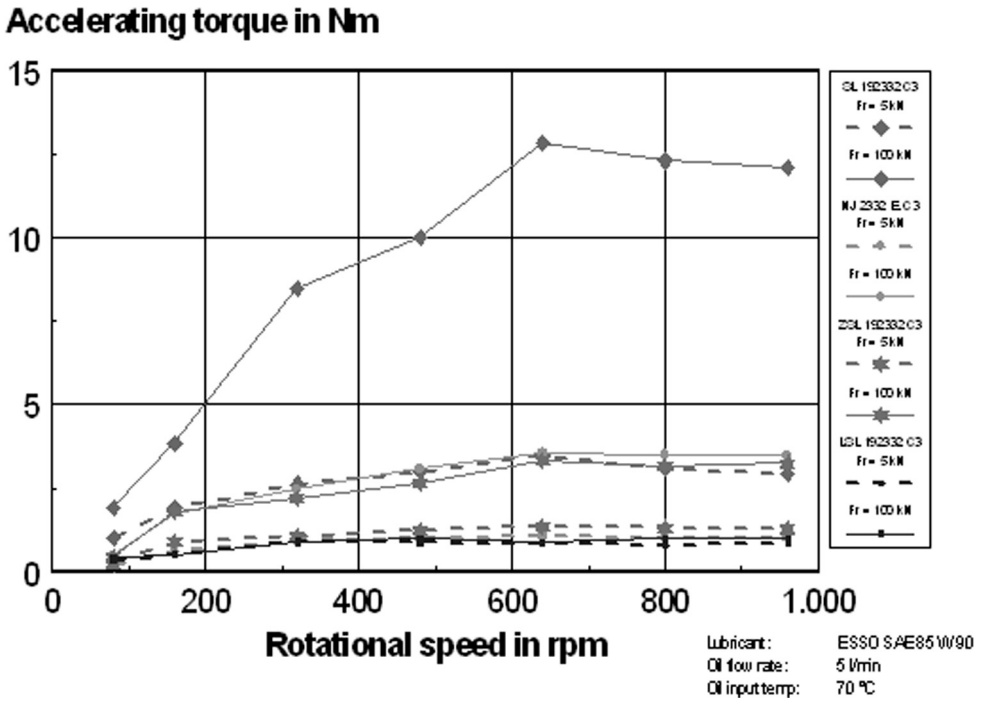

Fig. 14: Accelerating power of a rolling element (equation 9)

The power determined by these abrupt acceleration processes can reach up to 1000 W. As a result it can be shown that because of these high acceleration power values the lubrication film can breakdown. It was found that these working conditions are especially critical for the smearing occurrence and the material transfer associated with these conditions are called “acceleration smearings”.

5.2 Correlation between Cage and Rolling Element Speed

When considering the dependence between the inner ring, roller set or cage speed and the speed of a rolling element and applying the derived equations from chapter 3.1.3 a correlation was found between the roller set or cage slip and the slip of the rolling element .
Figure 15 illustrates the variation in $S_{C,meas.}/S_{C,work}$, which corresponds to the correlation between the roller set or cage slip and the rolling element slip within the load zone. The deviation between the calculated and measured values is max. ± 5 %. A deviation of 5 % results in a slip difference of approximately 0.5 % between the measured and calculated slip values at lower speeds.

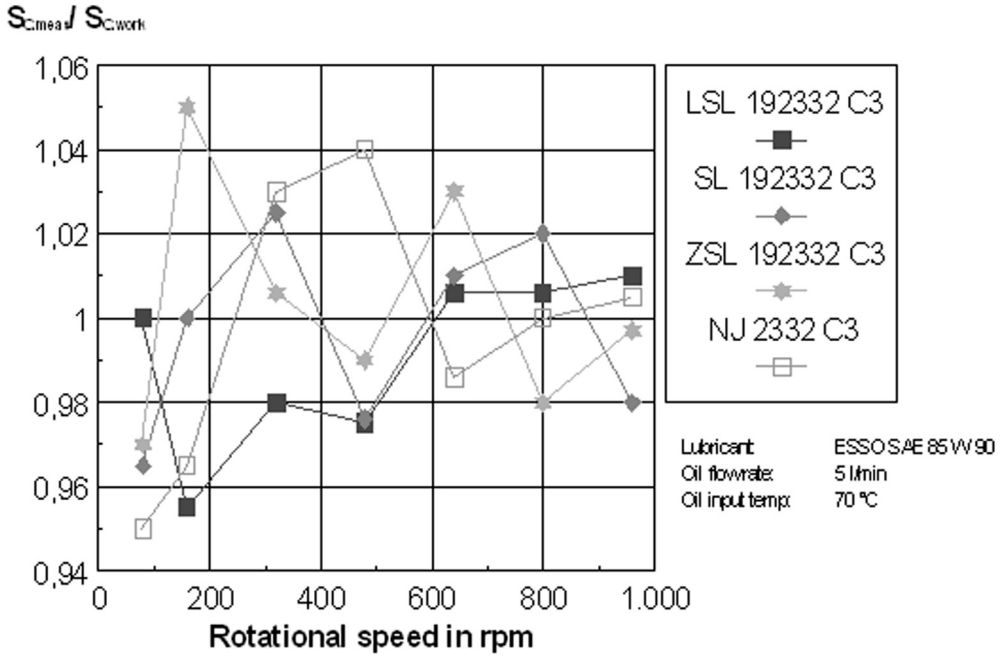

Fig. 15: Correlation between rolling element slip and slip of the roller set or cage

5.3 Smearing Behaviour

From the tests to examine the bearing kinematics it was known that no smearing occurs after running in a cylindrical roller bearing. New SL bearings are capable of reproducing smearing, load value and direction have a significant influence on the kinematic behaviour of a bearing.
For testing the initial limits of cylindrical roller bearings a test program was carried out. As more bearings were tested (approximately 30) the consistency of the results was proved. It was found that with new full complement cylindrical roller bearings having a rotational speed characteristic of $n_{IR}/n_G = 0.6$, smearing will occur independent of the applied load (for load zone situated above the bearing). These results have been confirmed by further tests with new full complement bearings. Additionally, for loads acting vertically upwards, it was found that there is no occurrence of smearing through the investigated speed range of $n_{IR}/n_G = 0.1$ to 1.2. Therefore, new full complement cylindrical roller bearings should be fitted in the speed range $n/n_G < 0.6$ in order to eliminate smearing, regardless of the applied load and the load direction.
Further tests have been conducted in order to extend the working area of full complement cylindrical roller bearings up to their limiting speed n_G. Therefore tests using several coatings, e.g. black oxide, chromium and

phosphate have been carried out to develop the most effective coating. To prove this the " smearing occurrence tests " which are tests for load zone against the direction of gravity, speeds of 480 and 960 rpm and radial loads of 5 and 100 kN, have been conducted. It was found that the tested coatings show good prevention against smearing. However, taking into account the production costs, the black oxide have been established as the most effective coating.

Therefore, extensive tests using black oxide raceway coatings have been performed over the complete speed range with the result that a black oxide coating not only prevents smearing but also the frictional torque has been reduced by up to 10 or 20% when applied to new full complement cylindrical roller bearings.

5.4 Application of the Results

The results obtained from these tests, according to the frictional torque and kinematics, have been applied to the INA development of a bearing simulation program "Simpl" [12], where the test results have been used to verify the program and thus apply it to other bearing sizes and types. The program uses the known values for friction energy W_K (6) to calculate the smearing danger. Using these known values, the load and relative speed in conjunction with instantaneous motion characteristics of the rolling elements are taken into consideration because the decisive conditions for smearing are whether the rolling element will be accelerated from a point without any rotation or whether the rolling elements are already rotating before beginning the acceleration.
With these tools INA is able, not only for full complement cylindrical roller bearings but also other bearing sizes and designs, to calculate the respective friction torque, kinematics and smearing danger.
In figures 16 and 17 examples of different bearing designs (SL 192332 and LSL 192332) are shown at the same working point (load zone above, load 5 kN, speed 960 rpm) with the associated smearing danger. The smearing occurrence is investigated as a calculated local energy of acceleration of 10 to 15 W. As it can be seen in figure 16 the smearing danger of an uncoated full complement cylindrical roller bearing (size SL 192332) is very high and figure 17 shows no smearing danger for the brass disc cage bearing series LSL 192332.

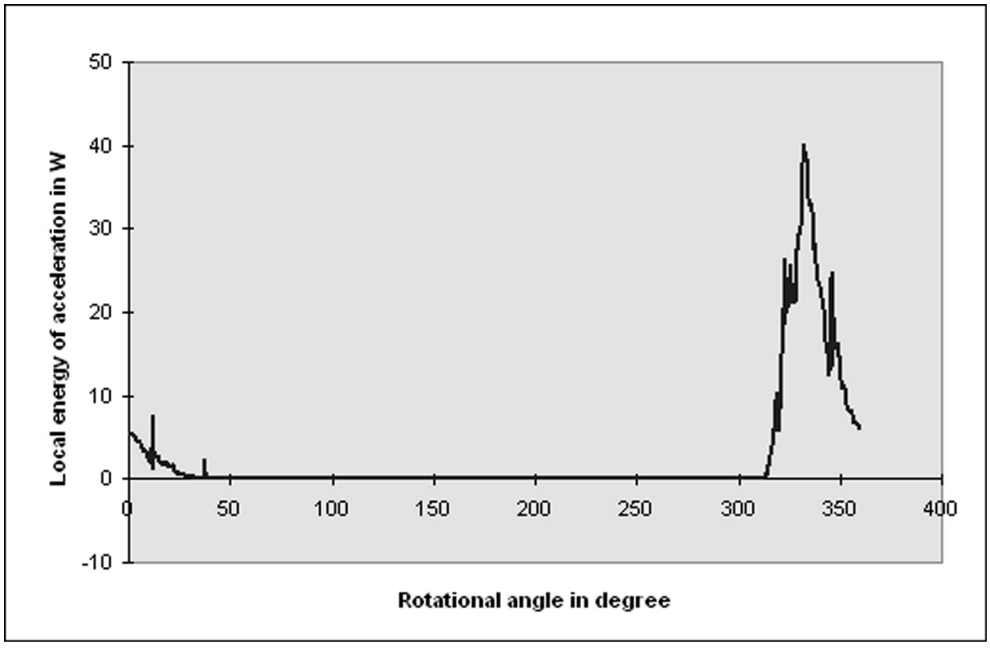

Fig. 16: Local energy of rolling element acceleration W_A - SL 192332

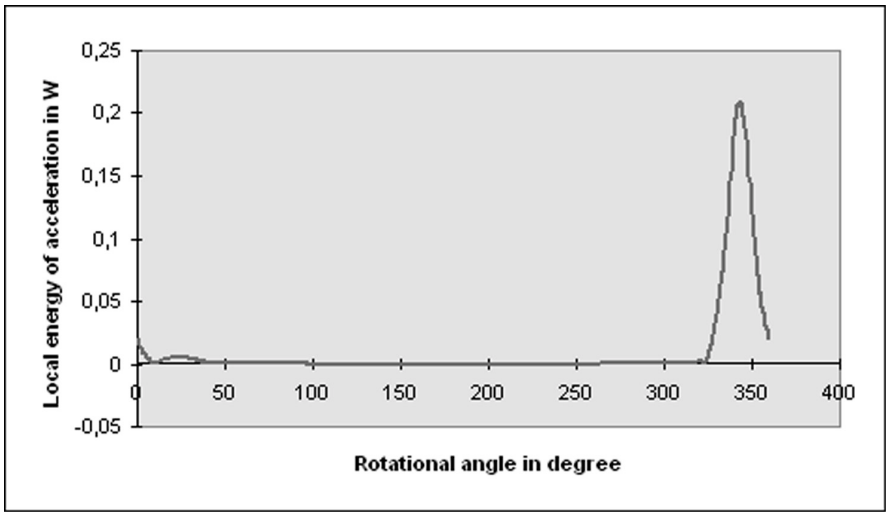

Fig. 17: Local energy of rolling element acceleration W_A - LSL 192332

6. CONCLUSION

The tests have shown that the rotational speed of the rolling elements in the different rotational speed zones in a cylindrical roller bearing have been essentially influenced by the internal bearing design with respect to the design of the cages.
Furthermore it was evaluated that under constant working conditions the roller set or cage rotational speeds correlate with the rolling element rotational speed in the load zone.
An important result obtained from the tests showed that the speed difference of the rolling elements, and hence the rolling element slip, has an essential influence on the condition of smearing. The applied bearing load has little influence on the smearing.
It was found that by using black oxide raceway coatings, the permitted working area according to the speed limit of full complement cylindrical roller bearings was extended to the limiting speed n_G which is stated in the INA catalogue.

7. ACKNOWLEDGEMENT

The authors appreciate the cooperation given by the INA Company and the Georg-Simon-Ohm-Fachhochschule Nürnberg.

8. REFERENCES

1. INA Bearings: Main Catalogue of bearing manufacturer INA, 2000
2. Harris, T. A.: Rolling Bearing Analysis, Third Edition, John Wiley & Sons, INC, 1991
3. Kaufmann, H. N. and Walp, H. O.: Interpreting Service Damage in Rolling Type Bearings, Chicago, ASLE 1958
4. Hamer,J. C., Sayles, R. S., Ioannides, E,: An experimental investigation into the boundaries of smearing failure in roller bearings, Trans. of the ASME, Paper No. 89 – Trib. –54, 1989
5. Hilscher, G.: Smearing in bearings – a contribution in order to solve the problem theoretically and experimentally, (Anschmierungen bei Wälzlager – ein Beitrag zur theoretischen und experimentellen Lösung des Problems), PhD thesis Erlangen, 1989
6. Wadewitz, M.: Reasons for smearing at the rolling/sliding contact, (Ursachen der Anschmierungen im Wälz-/Gleitkontakt), PhD thesis Erlangen, 1993
7. Eglinger, M.: Influence of lubrication and rolling element surface on the formation of smearing, (Einfluß des Schmierstoffes und der Rollenbeschaffenheit auf die Entstehung von Anschmierungen), PhD thesis Erlangen, 1995
8. Scherb, B. J. and Giese, P.: Smearing Behaviour of full complement Cylindrical Roller Bearing (Original title: Anschmierverhalten vollrolliger Zylinderrollenlager), German Journal: Antriebstechnik 33, 1994
9. Brändlein, Eschmann, Hasbarger, Weigand: Roller Bearing Theory (Original title: Die Wälzlagerpraxis) Handbook for Calculation and Design of Bearings, third Edition, Vereinigte Fachverlage GmbH, Main, 1995.
10. Lippert, R. and Scherb, B. J.: Low Friction Cylindrical Roller Bearings (Original title: Reibungsarme Zylinderrollenlager), German Journal: Antriebstechnik 32, 1993.
11. INA Bearings: Bearing Simulation Program „Simple“.
12. Scherb, B. J.: Correlation between cage and rolling element speed in a cylindrical roller bearing, (Original title: Zusammenhang zwischen Käfig – und Wälzkörperdrehzahl bei Zylinderrollenlagern), German Journal: Antriebstechnik 36, 1997